Chemical Science

ROYAL SOCIETY OF CHEMISTRY

EDGE ARTICLE

View Article Online
View Journal | View Issue

Cite this: *Chem. Sci.*, 2025, **16**, 16347

All publication charges for this article have been paid for by the Royal Society of Chemistry

Received 3rd June 2025
Accepted 1st August 2025

DOI: 10.1039/d5sc04010h

rsc.li/chemical-science

Sunlight-driven photoinduced electron/energy transfer-reversible addition-fragmentation chain transfer polymerization at a large scale

Zi-Hui Fan,†[a] Wei-Wei Fang,†[ab] Yi-Xing Liu,[a] Zheng-Hao Xiao,[c] Jian-Kun Yu,[a] Xu-Yi He,[d] Xian-Zhen Wang,[a] Xue-Ning Tang,[e] Lei Xia,*[a] Long-Xiang Tang*[a] and Tao He *[a]

Photoinduced electron/energy transfer-reversible addition-fragmentation chain transfer (PET-RAFT) polymerization is a sustainable and powerful tool to synthesize polymers and copolymers. However, the development of large-scale production and polymerizations using sunlight irradiation remain top challenges for PET-RAFT polymerizations. In this study, conjugated cross-linked phosphine (PPh_3-CHCP) was explored as a heterogeneous photocatalyst for efficient PET-RAFT polymerization. This development allowed PET-RAFT processes to achieve high monomer conversions, low dispersity and good chain-end fidelity under a broad range of wavelengths and sunlight irradiation from various monomers. The heterogeneous PPh_3-CHCP photocatalyst could be easily separated and reused without obvious structural deterioration or decrease in efficiency. Sunlight-driven photopolymerization of MA (methyl acrylate) was scaled up to 2 L (conversion of 93%), and the obtained polymer showed good control over both molecular weight and dispersity ($Đ = 1.13$). White light-driven polymerization of MA (conversion of 91%, $Đ = 1.27$) reached a 6 L scale. These results demonstrate a great potential for industrial applications.

Introduction

Reversible-deactivation radical polymerizations (RDRPs) have emerged as a versatile and useful method to prepare well-defined polymeric materials.[1,2] Recently, efforts have been made to employ light as an energy source for RDRPs, as it allows spatiotemporal control over polymerization, and provides an alternative avenue for polymer synthesis through green and sustainable processes.[3,4] In these polymerizations, photocatalysts converted photon energy into chemical energy and triggered the generation of propagating radicals, which played a critical role. Up to the present, various photocatalysts and related photo-RDRPs have been developed, such as photocatalyzed atom transfer radical polymerization (photo-ATRP), photoinduced electron/energy transfer-reversible addition-fragmentation chain transfer (PET-RAFT) polymerizations, *etc.*[5–9] Compared with photo-ATRP, especially photoinduced metal-catalyzed ATRP, PET-RAFT does not need to use or only uses a tiny amount of toxic metal complexes,[10,11] which makes the purification of the obtained polymers much easier and more convenient to be applied in industry.

In recent PET-RAFT studies, great progress has been made in enhancing polymerization efficiency and versatility.[12,13] However, although it is highly desired by industry, there is relatively slow progress in developing large-scale PET-RAFT due to typical barriers. For example, the light intensity needs to be greatly increased to overcome the adverse effects which are derived from the light absorption of reactants or light scattering of heterogeneous photocatalysts in large-scale synthesis.[14] It was reported that combination with flow devices offered an opportunity to develop scale-up PET-RAFT, as the high surface-area-to-volume ratio of the photoreactor was beneficial to mass transfer and light penetration.[15] However, negative features such as deviation of prepared polymers and undesired side reactions were observed, especially when extending the reactor length, residence time, or raising the monomer concentration.[16,17] Up to the present, the scale of most PET-RAFTs has been below 200 mL.[18,19]

[a]*School of Chemistry and Chemical Engineering, Anhui Province Key Laboratory of Value-Added Catalytic Conversion and Reaction Engineering, Anhui Province Engineering Research Center of Flexible and Intelligent Material, Hefei University of Technology, Hefei, Anhui 230009, P. R. China. E-mail: lxia@hfut.edu.cn; tanglx@hfut.edu.cn; taohe@hfut.edu.cn*

[b]*School of Chemistry and Chemical Engineering, Key Laboratory of Material Chemistry for Energy Conversion and Storage Ministry of Education, Hubei Key Laboratory of Material Chemistry and Service Failure, Huazhong University of Science and Technology, Wuhan, Hubei 430074, P. R. China*

[c]*School of Microelectronics, Microelectronics Science and Engineering, Southern University of Science and Technology, Shenzhen, Guangdong 518005, P. R. China*

[d]*University of Science and Technology of China, Hefei, Anhui 230026, P. R. China*

[e]*School of Data Science, The Chinese University of Hong Kong, Shenzhen, Guangdong 518172, P.R. China*

† Z. H. F and W. W. F contributed equally to this work.

Sunlight is an inherently abundant high-intensity light source, and sunlight-driven polymerizations are undoubtedly valuable for green and sustainable scale-up production. However, successful sunlight-driven PET-RAFT is very challenging. One of the typical reasons is that the high illumination intensity of sunlight (higher than 1000 W m^{-2}) may result in the irreversible deterioration of excited molecules.[20–22] Meanwhile, the high-energy photons in the solar spectrum could also lead to undesirable side reactions (*e.g.* self-initiation of monomers and degradation of polymers containing unstable groups in main chains). As a result, the scale of most sunlight driven PET-RAFTs was less than 3 mL. The photocatalysts applied in current PET-RAFTs mainly include homogeneous (*e.g.* dyes and related compounds, organocatalysts, *etc.*)[23–27] and heterogeneous (*e.g.* bioactives,[28] nanoparticles (NPs),[29–32] metal organic frameworks,[33–35] covalent organic frameworks,[36,37] carbon-based nanomaterials,[38–40] nanocomposites[41,42]) materials. Heterogeneous photocatalysts attract widespread interest for their facile recycling, minimal catalyst requirements (*e.g.* EY-SNP, 3 ppm),[43] excellent tolerance to oxygen, *etc.* Although these photocatalysts could be applied in polymerizations under different light irradiations (*e.g.* UV (ultraviolet), blue, green, red, NIR (near infrared) and white), potential photobleaching makes most molecular photocatalysts lack the capability of long-term operation under sunlight irradiation. Meanwhile, for most of the photocatalysts utilized in sunlight-driven photopolymerizations, it is challenging to achieve ideal monomer conversions (*e.g.* >90%) within a short period (*e.g.* 6–8 hours).[41,44] Although carbon nanodots and Ag_2S nanocrystals can offer polymers with high conversions and well-controlled molecular weights, the purification is relatively complicated due to their nanoscale size.[31,38] Other heterogeneous photocatalysts such as Ag_3PO_4 NPs and zirconium-porphyrin frameworks (ZrPHPs) could facilitate nearly quantitative monomer conversions, but they lead to relatively broad dispersity of the synthesized polymers or narrow choice of monomers.[29,35]

Ideally, a photocatalyst applied in large-scale sunlight-driven PET-RAFT should have a high absorption coefficient in visible and NIR range, in order to enhance photon penetration and avoid competitive absorption of reactant. The photocatalyst should also have suitable redox potential to reduce the chain transfer agent and regulate the reversible deactivation process. Although great progress has been made in PET-RAFT recently, the development of stable materials and efficient methodology to employ sunlight directly in large-scale synthesis with good control over the polymer's molecular weight and dispersity has remained a big challenge. This is clearly an area worth exploring, keeping in view the potential for practical industrial applications, together with the green and sustainable nature.

π-Conjugation extension as well as the introduction of halogens were the most applied guiding principles for designing long-wavelength-absorbing photocatalysts.[45] Additionally, benefiting from the extended conjugated network which provides a pristine site for carrier transport, heterogeneous photocatalysts (*e.g.* TPP-ImBr-CPP,[46] TAPPY-DTDD-CMP,[47] TCPP-TPDA-COF[48]) showed enhanced electron transfer capability under light irradiation, which offered a robust platform for the development of PET-RAFT polymerization. Previously, we reported the synthesis and applications of PPh_3-CHCP in photo-ATRP.[49] With the deep understanding of the PET-RAFT polymerization mechanism and continuing investigation of rational design of photocatalysts, herein, we suggest that PPh_3-CHCP, being constructed by crosslinked phosphine and substituted aromatic group (Fig. S1), may serve as an efficient photocatalyst for PET-RAFT. This is because it shows moderate photocatalytic activity under visible light irradiation. In this work, PPh_3-CHCP served as a photocatalyst for PET-RAFT polymerization, achieving high monomer conversion and controllable molecular weight properties under varying light irradiation including sunlight. The heterogeneous nature of PPh_3-CHCP enables it to maintain photocatalytic performance after multiple recycling processes. White light-driven polymerization of MA (methyl acrylate) (conversion of 91%, $Đ = 1.27$) reached a 6 L scale. In addition, sunlight-induced PET-RAFT could be successfully conducted at a 2 L scale (Fig. 1a), which

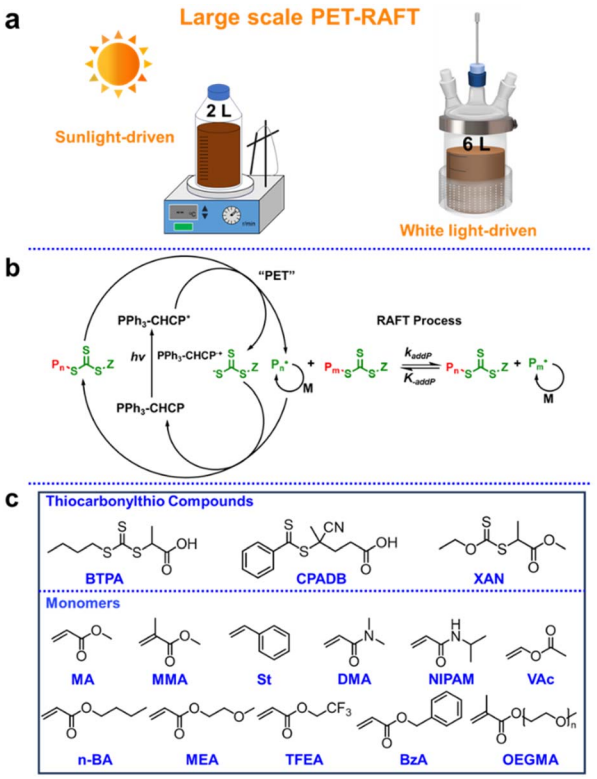

Fig. 1 Development of photocatalyst for large-scale PET-RAFT. (a) Large-scale PPh_3-CHCP-catalyzed PET-RAFT polymerization (2 L reaction scale of PMA under sunlight irradiation and 6 L reaction scale of PMA under white-light irradiation). (b) Mechanism of PPh_3-CHCP-catalyzed PET-RAFT polymerization. (c) List of RAFT agents and monomers investigated in this study. MA (methyl acrylate), MEA ((2-methoxyethyl) acrylate), BzA (benzyl acrylate), *n*-BA (*n*-butyl acrylate), TFEA (2,2,2-trifluoroethyl acrylate), MMA (methyl methacrylate), OEGMA (poly(ethylene glycol) methyl ether methacrylate), NIPAM (*N*-isopropylacrylamide), DMA (*N*,*N*-dimethylacrylamide), St (styrene), and VAc (vinyl acetate). BTPA (2-(((butylthio)carbonothioyl)thio)propanoic acid), CPADB (4-cyano-4-(phenylcarbonothioylthio)pentanoic acid), XAN (2-(ethoxythioxomethylthio)propionic acid methyl ester).

produced PMA with 93% conversion and good control over dispersity ($Đ$ = 1.13), demonstrating its great potential for industrial applications.

Results and discussion

PPh_3-CHCP-catalyzed PET-RAFT polymerizations under blue-light irradiation

The typical characterizations of the PPh_3-CHCP photocatalyst were consistent with our previous report, indicating the successful construction (Fig. S2–S9). Further cyclic voltammetry investigation of PPh_3-CHCP exhibited a reduction potential of (E_{ox}* = −1.35 V) (Fig. S10), indicating that excited states of PPh_3-CHCP were highly reducing to reduce BTPA (2-(((butylthio) carbonothiolyl)thio)propanoic acid) (E_{red} = −0.6 V) and CPADB (4-cyano-4-(phenylcarbonothioylthio)pentanoic acid) (E_{red} = −0.4 V).[50]

The photocatalytic performance of PET-RAFT polymerization using PPh_3-CHCP was first evaluated under blue-light irradiation (λ_{max} = 465 nm, 2 mW cm^{-2}), with MA as model monomer and BTPA as CTA (chain transfer agent) (Fig. S11 and S12). Polymerization of deoxygenated MA (freeze–pump–thaw) achieved 97% monomer conversion within 9 hours (Table 1, entry 3), and the molecular weight of PMA (M_n = 17 000, $Đ$ = 1.07) was close to the theoretical value, indicating good control of the polymerization. Applying nitrogen bubbling instead of freeze–pump–thaw as prior deoxygenation process could achieve similar results (Table S1), which might be beneficial for potential industrial applications.

The results of the kinetic study are shown in Fig. 2. A linear dependence of $\ln([M]_0/[M]_t)$ with the exposure time corresponds to pseudo-first-order polymerization kinetics (Fig. 2a), suggesting a constant concentration of propagating radicals in the polymerization systems. PPh_3-CHCP in DMSO exhibited an induction period (<2 h), which might be due to the presence of dissolved trace amount of oxygen in the reaction solutions.[38] The experimental molecular weight (MW) values increased linearly with monomer conversion, which were in good agreement with the theoretical values. In addition, the dispersity decreased as the monomer conversion increased, and a narrow MW distribution ($Đ$ < 1.09) was finally obtained (Fig. 2b), corresponding to a controlled radical polymerization nature. Under blue-light irradiation (2 mW cm^{-2}), an apparent polymerization rate constant (k_{app}) of 0.47 h^{-1} was observed. The $k_{p,app}$ for polymerization of MA using PPh_3-CHCP was close to that using ZnTPP (0.67 h^{-1}),[50] but lower than that using fac-[Ir(ppy)$_3$] (2.30 h^{-1}).[10] The SEC (size exclusion chromatography) curves of PMA obtained in the kinetics study showed a unimodal distribution of MW shifting with the exposure time (Fig. 2c).

Temporal control over polymerization was investigated by intermittent off/on switching of the light (Fig. 2d and e). As expected, switching off the light completely ceased the polymerization. The dark period was prolonged up to 12 hours, and a negligible monomer conversion was observed, suggesting that active radicals were not efficiently generated under dark conditions (Fig. S13). Switching back on the light source resumed the linear chain propagation, as suggested by the agreement between the theoretical and experimental molecular weights (M_n = 16 600, $M_{n,th}$ = 16 200) and low dispersity ($Đ$ = 1.08) of the resulting polymers (Fig. S14).

The ability to synthesize block copolymers was also investigated. Results from *in situ* chain extension experiments revealed the highly living nature of the resulting polymers. For instance, a PMA macroinitiator (conversion of 96%, M_n = 16 600, $Đ$ = 1.08) was employed to initiate the second monomer (MEA),

Table 1 PPh_3-CHCP-catalyzed PET-RAFT polymerizations[a]

Entry	Monomer	PPh_3-CHCP (mg mL^{-1})	[M]/[CTA]	Solvent	Time (h)	Conv. (%)	$M_{n,th}$	M_n	$Đ$
1	MA	2	50 : 1	DMSO	9	97	4400	4500	1.08
2	MA	2	100 : 1	DMSO	9	97	8600	8400	1.08
3	MA	2	200 : 1	DMSO	9	97	16 900	17 000	1.07
4	MA	2	400 : 1	DMSO	8	92	31 900	35 000	1.10
5	MA	2	1000 : 1	DMSO	6	90	77 700	75 800	1.17
6[b]	MA	1	1500 : 1	DMSO	12	91	117 700	105 200	1.16
7[b]	MA	0.75	2000 : 1	DMSO	12	85	146 600	143 800	1.17
8	MEA	2	200 : 1	DMSO	20	96	25 200	25 700	1.12
9	BzA	2	200 1	DMSO	20	98	31 900	29 400	1.10
10	*n*-BA	2	200 : 1	DMSO	11	90	22 900	24 200	1.06
11	TFEA	2	200 : 1	DMSO	20	92	28 400	26 600	1.06
12	MMA	0.5	200 : 1	DMSO	40	90	18 200	19 500	1.17
13	St	2	100 : 1	IPA	48	91	9700	10 500	1.13
14	OEGMA	2	100 : 1	Water	6	90	27 200	26 900	1.13
15	NIPAM	2	200 : 1	Water	24	80	18 300	18 100	1.08
16	DMA	2	200 : 1	Water	8	95	19 100	21 800	1.13
17	VAc	2	200 : 1	DMSO	24	50	8800	8000	1.14

[a] Polymerizations were performed under blue-light irradiation (2 mW cm^{-2}) at room temperature unless specified otherwise. Reaction conditions: entries 1–7, [MA]/[BTPA] = 50, 100, 200, 400, 1000, 1500, 2000/1 in 50 vol% DMSO. Entries 8–11, [M]/[BTPA] = 200/1 in 50 vol% DMSO. [MMA]/[CPADB] = 200/1 in 50 vol% DMSO. [St]/[BTPA] = 100/1 in 50 vol% IPA. Polymerization of styrene was conducted at 40 °C. [OEGMA]/[CPADB] = 100/1 in 75 vol% water. [NIPAM]/[CPADB] = 200/1 in 75 vol% water. [DMA]/[BTPA] = 200/1 in 50 vol% water. [VAc]/[XAN] = 200/1 in 50 vol% DMSO. DMSO (dimethyl sulfoxide), IPA (isopropanol). [b] 1 mW cm^{-2} blue-light irradiation.

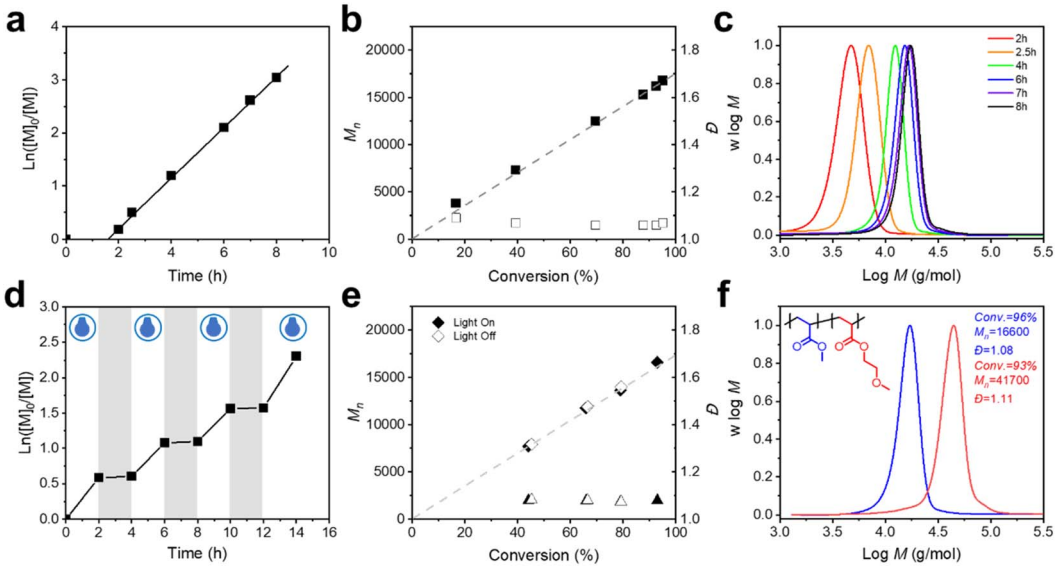

Fig. 2 Results for the polymerization of MA using PPh_3-CHCP photocatalyst. (a) Kinetics and (b) evolution of molecular weight (M_n, filled points) and dispersity ($Đ$, open points) as a function of monomer conversion in PET-RAFT polymerization of MA. (c) SEC traces of PMA synthesized in the kinetic study. (d) "ON/OFF" experiments catalyzed by PPh_3-CHCP under blue LED irradiation. (e) Plot of M_n and $Đ$ (filled symbols indicate after irradiation, and open symbols indicate after dark period) *versus* monomer conversions in "ON/OFF" experiments. (f) SEC traces of PMA and PMA_{200}-*b*-$PMEA_{200}$ block copolymer synthesized by *in situ* chain extension.

which resulted in 93% conversion and offered a well-defined di-block copolymer ($M_n = 41\,700$, $Đ = 1.11$, Fig. 2f). In accordance with the aforementioned experimental procedures, both the ABAB quadri-block copolymer (PMA-*b*-PMEA-*b*-PMA-*b*-PMEA) and the ABC tri-block copolymer (PMA-*b*-PMEA-*b*-Pn-BA) were successfully synthesized (Fig. S15). Meanwhile, ^{1}H NMR analysis was applied to evaluate the chain-end fidelity of the obtained PMA ($M_n = 8800$, $Đ = 1.06$). The ratio of integral value between methine group and methyl group from the CTA was 0.82 : 3, which was close to the theoretical ratio (1 : 3) (Fig. S16a). Furthermore, we performed ultraviolet/visible analysis on the synthesized PMA. The absorption peak at $\lambda = 443$ nm for the PMA chain end closely matches that of the pristine BTPA RAFT agent, confirming high retention of the RAFT end-group functionality under our experimental conditions (Fig. S16b).

The scope of PPh_3-CHCP-catalyzed PET-RAFT could be extended to a variety of monomers. In all cases, well-defined polymers with low dispersity ($Đ < 1.17$) and high monomer conversions were obtained (Table 1 and Fig. S17). When styrene (a typical low-k_p monomer) was applied, 91% conversion and polymers with a dispersity of 1.13 could still be achieved (Table 1, entry 13). Water-soluble monomers including OEGMA, NIPAM and DMA were also polymerized in water, achieving monomer conversion of 90%, 80%, and 95%, with dispersity of 1.13, 1.08, and 1.13 of the produced polymers respectively. Polymerization of unconjugated monomers such as vinyl acetate (VAc) was also conducted and achieved 50% monomer conversion (designed DP : 200) with relatively low dispersity (1.14) in 24 h (Table 1, entry 17), indicating that PPh_3-CHCP-catalyzed PET-RAFT polymerizations was also applicable for low-activity monomers. This system also enabled synthesis of polymers with varying degree of polymerization (DP) (targeted from 50 to 2000) (Table 1 and Fig. S18). For example, PMA with DP of 2000 and a dispersity of 1.17 could be easily obtained with a conversion at 85% within 12 hours. A further increase in the monomer conversion to 92% would result in a broader dispersity of 1.25 (Fig. S19), which might be attributed to the low diffusion of the heterogeneous photocatalyst in highly viscous reaction mixture (especially at high monomer conversion) resulting in reduced deactivation process. These results suggested the high flexibility of PPh_3-CHCP-catalyzed PET-RAFT polymerization.

PET-RAFT under sunlight irradiation and large-scale production

As PPh_3-CHCP exhibited strong absorption under broadband light irradiation, PPh_3-CHCP-catalyzed PET-RAFT polymerization could be extended to green-($\lambda_{max} = 525$ nm, 2 mW cm^{-2}), orange-($\lambda_{max} = 590$ nm, 2 mW cm^{-2}), and white-light (2 mW cm^{-2}) irradiation. All polymerizations achieved ≥93% monomer conversion and yielded polymers with a low dispersity of 1.07 (Fig. 3a and Table S2). We point out that the reaction time was longer than that for blue light. This might be due to the weaker absorption of PPh_3-CHCP in green-, orange- and white-light regions.

More importantly, the wide absorption of PPh_3-CHCP was beneficial to utilize the solar spectrum directly, which covers wavelengths from 250 to 2500 nm. We applied a xenon lamp to simulate sunlight, and the reaction kinetics are shown in Fig. 3b and c. There was a linear dependence of $\ln([M]_0/[M]_t)$ with exposure time and the experimental MW values increased linearly with monomer conversion (Fig. S20). Subsequently, various monomers were applied to evaluate the compatibility of

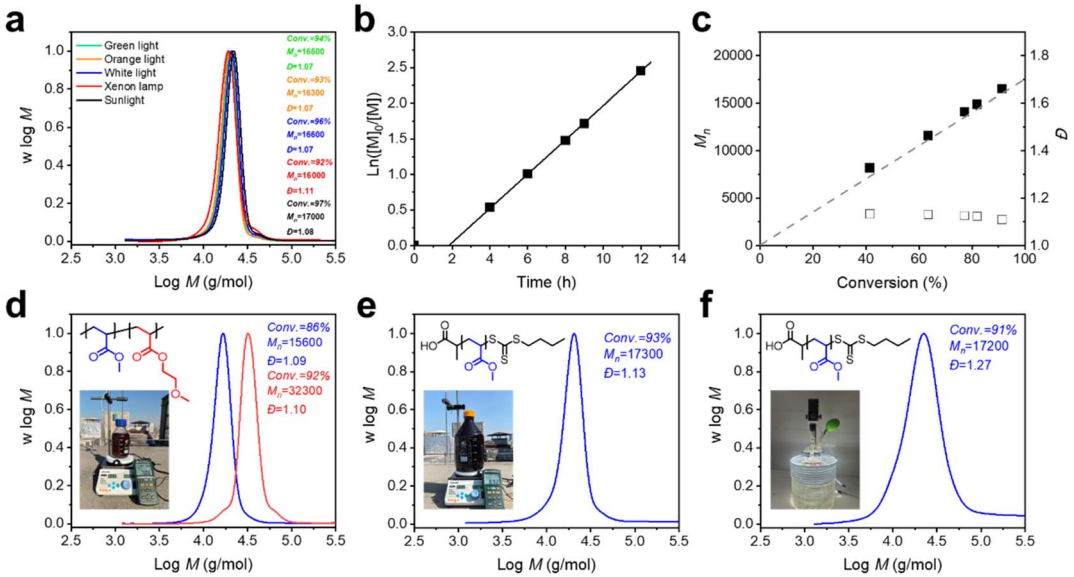

Fig. 3 PET-RAFT polymerizations under broadband lights and sunlight irradiation. (a) SEC traces of PMA synthesized using PPh_3-CHCP as a photocatalyst under green, orange, white, xenon lamp and sunlight irradiation. (b) Kinetics and (c) evolution of molecular weight (M_n, filled points) and dispersity ($Đ$, open points) in PET-RAFT polymerization under xenon lamp (80 mW cm^{-2}). (d) SEC traces of 250 mL scale of PMA macroinitiator (in blue) and 500 mL scale of PMA_{200}-*b*-$PMEA_{136}$ block copolymer (in red) synthesized using PPh_3-CHCP under sunlight irradiation. (e) SEC trace of 2 L scale of synthesis using PPh_3-CHCP under sunlight irradiation. (f) SEC trace of 6 L scale of PMA synthesized using PPh_3-CHCP under white-light irradiation. Reaction conditions: [M]/[BTPA] = 200/1 in 50 vol% DMSO. PPh_3-CHCP = 2 mg mL^{-1}.

the PPh_3-CHCP-catalyzed PET-RAFT system under sunlight irradiation (variation of solar radiation and reported temperature are supplied in Fig. S21). Polymerizations of MA, MEA, BzA, *n*-BA and MMA were successfully performed, resulting in monomer conversions of 97%, 97%, 98%, 91%, and 80% within 8 hours respectively (Table S3 and Fig. S22). The M_n of obtained polymers were close to their theoretical values, and low dispersity (1.08, 1.10, 1.10, 1.14 and 1.19, respectively) was obtained. The monomer conversion was relatively low for MMA, which may be due to its low activity. These results strongly suggested that PET-RAFT polymerizations could be successfully performed under sunlight irradiation in the presence of PPh_3-CHCP. Polymerization was also performed without the photocatalyst under sunlight irradiation, as the UV light and blue light in the solar spectrum might trigger photoiniferter RAFT-type polymerization. Negligible conversion of MA was observed under xenon lamps, while ~43% conversion was achieved under sunlight irradiation (Table S4), indicating that high-energy photons in sunlight might trigger the fast photoiniferter initiation process at high ambient temperature and boost PET-RAFT polymerization.

Then, large-scale PPh_3-CHCP-catalyzed PET-RAFT polymerization was performed under sunlight. For instance, after 8 hours of sunlight irradiation, a 500 mL scale of polymerization mixture (comprising 250 mL of MA and 250 mL of DMSO) offered 86% monomer conversion, yielding PMA with a dispersity of 1.09 (Fig. 3d). In addition, a block copolymer could also be prepared at large scale. 250 mL of MEA solution (V_{MEA}/V_{DMSO} = 1/1) was *in situ* fed into a 500 mL vial containing 250 mL of prepared PMA macroinitiator solution from sunlight irradiation. After 8 hours of blue-light irradiation, well-defined di-block copolymer PMA-*b*-PMEA (M_n = 32 300, $Đ$ = 1.10) was obtained (conversion: 92%). There was no obvious difference in molecular weight and dispersity of prepared polymers between the large-scale system and the small vial, and this suggested the robustness and reproducibility of this development.

To further investigate the scalability of the PPh_3-CHCP-catalyzed PET-RAFT polymerization system, 2 L scale of MA (V_{MA}/V_{DMSO} = 1/1) was used under sunlight irradiation (24 h), yielding PMA with a dispersity of 1.13 (conversion: 93%, M_n = 17 300) (Fig. 3e). Scaled-up PET-RAFT polymerization under continuous light irradiation was also evaluated, and reached 91% monomer conversion after 48 h white-light irradiation at a 6 L scale (Fig. 3f). To the best of our knowledge, these are the largest-scale PET-RAFT polymerizations using sunlight and white light to date. The successful large-scale synthesis of both homopolymers and block copolymers demonstrates great industrial application potential.

Reusability and proposed mechanisms

As a heterogeneous catalyst, PPh_3-CHCP could be easily separated from the reaction mixture and reused in multiple polymerization cycles while retaining its high photocatalytic efficiency. After 5 cycles, near-quantitative monomer conversions were still obtained, offering polymers with well-controlled molecular weights and low dispersity values (Fig. 4a and b). We also performed gravimetric analysis of PPh_3-CHCP after each recycling cycle. The results indicate an average catalyst recovery yield of ~90% per cycle (corresponding to ~10% mass loss) (Fig. S23), attributed to unavoidable mechanical losses during the recycling process. As normal photocatalysts usually

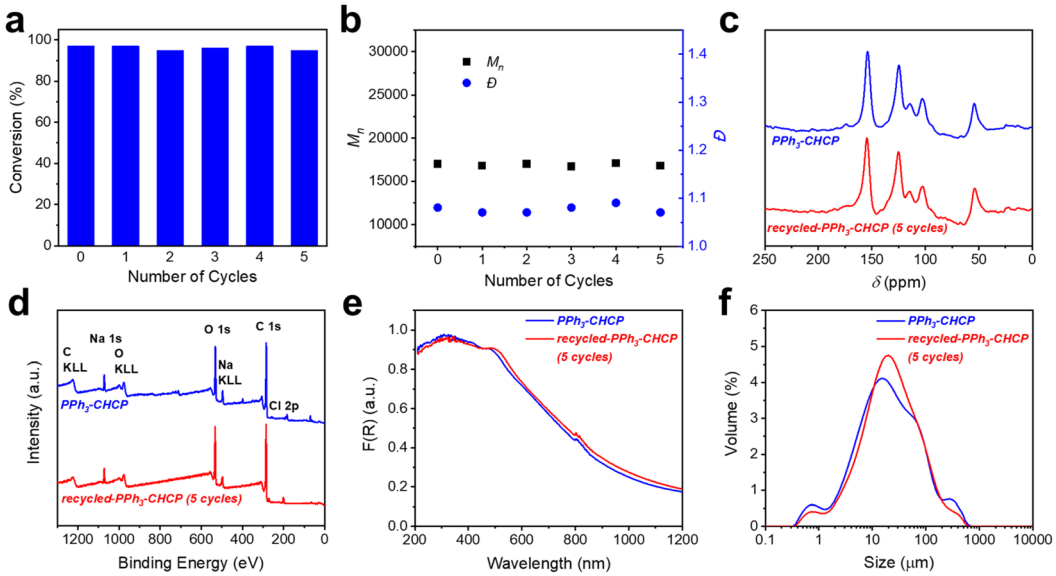

Fig. 4 Results for recycled PPh_3-CHCP photocatalyst after multiple cycles. (a) Monomer conversion and (b) molecular weight (M_n, squares) and dispersity ($Đ$, circles) of the resulting polymers in recycling experiments. (c) Solid-state CP/MAS ^{13}C NMR spectra, (d) relative XPS survey spectra, (e) solid-state UV-visible diffuse reflectance and (f) size distribution of PPh_3-CHCP before and after recycling experiments (5 cycles). Reaction conditions: [MA]/[BTPA] = 200/1 in 50 vol% DMSO under blue-light irradiation (2 mW cm^{-2}), PPh_3-CHCP = 2 mg mL^{-1}.

decompose under long-time light irradiation, herein, the photostability of recycled PPh_3-CHCP was further evaluated and the related results are shown in Fig. 4c–f, S24 and S25. No changes in structure, photophysical performance, morphology or size distribution were observed, which demonstrated the good stability under low-intensity photocatalytic reaction without using an electron donor. Furthermore, we compared the polymerization kinetics using the photocatalyst before and after 5 recycle experiments. The $k_{p,app}$ for polymerization of MA using 5-times recycled PPh_3-CHCP (0.21 h^{-1}) was similar to that of initial PPh_3-CHCP under xenon lamp irradiation (0.24 h^{-1}), indicating the high retention of photocatalytic activity after the recycling process (Fig. S26).

As a highly efficient PET-RAFT system, we proposed the oxidative quenching mechanism to elucidate the PPh_3-CHCP-catalyzed PET-RAFT polymerization (Fig. 1b). The photo charge transfer reaction occurred between CTA and the excited PPh_3-CHCP under light irradiation, generating initiating radicals and oxidized PPh_3-CHCP (PPh_3-CHCP$^{\bullet+}$). This was supported by fluorescence quenching study of the electron transfer between PPh_3-CHCP and RAFT agent (Fig. S27), where a continuous decrease in emission intensity was observed on increasing the concentration of the RAFT agent. The initiating radicals could either participate in the addition of vinyl monomer or regenerate PPh_3-CHCP while being deactivated.

Conclusions

In summary, a phosphine-based crosslinked polymer (PPh_3-CHCP) was exploited as a versatile and recyclable photocatalyst for PET-RAFT polymerization of various monomers under broadband light and sunlight irradiation. Polymers with precisely controlled molecular weight properties and high monomer conversions were achieved under varying light irradiation. PPh_3-CHCP was easily separated and reused in subsequent polymerizations without a decrease in photocatalytic efficiency. PPh_3-CHCP enabled successful sunlight-driven polymerization reactions at a 2 L scale, and white light-driven polymerization at a 6 L scale, which are the largest scales of sunlight-driven and white light-driven PET-RAFT polymerizations reported to date. We anticipate that this PPh_3-CHCP platform will provide a feasible solution for large-scale PET-RAFT production, highlighting great potential for industrial applications.

Author contributions

T. H., Z. H. F., and W. W. F. conceived the study. Z. H. F. performed the synthesis and characterizations. Y. X. L. carried out the electrochemical measurements. Z. H. X., J. K. Y., X. Y. H., X. Z. W., and X. N. T. discussed the results. W. W. F., L. X., L. X. T., and T. H. supervised the project, acquired funding for the research, and together with Z. H. F. wrote the manuscript.

Conflicts of interest

There are no conflicts to declare.

Data availability

Dataset: **https://doi.org/10.6084/m9.figshare.29675291.v1**.

All the data supporting this article have been included in the main text and the SI. See DOI: **https://doi.org/10.1039/d5sc04010h**.

Acknowledgements

We gratefully acknowledge financial support from the National Natural Science Foundation of China (22171067, 22101275), Postdoctoral Fellowship Program of CPSF (no. GZC20240536), and Fundamental Research Funds for the Central Universities of China (no. PA2023GDSK0074, no. PA2025GDSK0080).

References

1 N. P. Truong, G. R. Jones, K. G. E. Bradford, D. Konkolewicz and A. Anastasaki, *Nat. Rev. Chem.*, 2021, **5**, 859–869.
2 N. Corrigan, K. Jung, G. Moad, C. J. Hawker, K. Matyjaszewski and C. Boyer, *Prog. Polym. Sci.*, 2020, **111**, 101311.
3 Y. Lee, C. Boyer and M. S. Kwon, *Nat. Rev. Mater.*, 2021, **7**, 74–75.
4 C. Aydogan, G. Yilmaz, A. Shegiwal, D. M. Haddleton and Y. Yagci, *Angew. Chem., Int. Ed.*, 2022, **61**, e202117377.
5 D. A. Corbin and G. M. Miyake, *Chem. Rev.*, 2021, **122**, 1830–1874.
6 H. Zhou, L. Zhang, P. Wen, Y. Zhou, Y. Zhao, Q. Zhao, Y. Gu, R. Bai and M. Chen, *Angew. Chem., Int. Ed.*, 2023, **62**, e202304461.
7 Z. Lu, R. Zhao, H. Yang, X. Fu, Y. Zhao, L. Xiao and L. Hou, *Angew. Chem., Int. Ed.*, 2022, **61**, e202208898.
8 J. Sobieski, A. Gorczyński, A. M. Jazani, G. Yilmaz and K. Matyjaszewski, *Angew. Chem., Int. Ed.*, 2025, **64**, e202415785.
9 Y. Lee, C. Boyer and M. S. Kwon, *Chem. Soc. Rev.*, 2023, **52**, 3035–3097.
10 J. Xu, K. Jung, A. Atme, S. Shanmugam and C. Boyer, *J. Am. Chem. Soc.*, 2014, **136**, 5508–5519.
11 C. Wu, N. Corrigan, C. H. Lim, K. Jung, J. Zhu, G. Miyake, J. Xu and C. Boyer, *Macromolecules*, 2019, **52**, 236–248.
12 S. A. Logan, Q. Fu, Y. Sun, M. Liu, J. Xie, J. Tang and G. G. Qiao, *Angew. Chem., Int. Ed.*, 2020, **59**, 21392–21396.
13 Y. Lee, Y. Kwon, Y. Kim, C. Yu, S. Feng, J. Park, J. Doh, R. Wannemacher, B. Koo, J. Gierschner and M. S. Kwon, *Adv. Mater.*, 2022, **34**, 2108446.
14 K. C. Harper, E. G. Moschetta, S. V. Bordawekar and S. J. Wittenberger, *ACS Cent. Sci.*, 2019, **5**, 109–115.
15 S. Cañellas, M. Nuño and E. Speckmeier, *Nat. Commun.*, 2024, **15**, 307.
16 Y. Zhou, Y. Gu, K. Jiang and M. Chen, *Macromolecules*, 2019, **52**, 5611–5617.
17 Z. R. Zhong, Y. N. Chen, Y. Zhou and M. Chen, *Chin. J. Polym. Sci.*, 2021, **39**, 1069–1083.
18 Y. Xiao, Z. Xia, W. Hu, B. Liu and C. Lü, *Small*, 2024, **20**, 2309893.
19 Z. Xia, B. Liu, Y. Xiao, W. Hu, M. Deng and C. Lü, *ACS Appl. Mater. Interfaces*, 2023, **15**, 57119–57133.
20 W. Yao, C. Zhang, X. Wang, Z. Zhang, X. Li and H. Di, *Energy Convers. Manage.*, 2018, **164**, 579–587.
21 P. Borah, S. Sreejith, P. Anees, N. V. Menon, Y. J. Kang, A. Ajayaghosh and Y. L. Zhao, *Sci. Adv.*, 2015, **1**, e1500390.
22 P. R. Denish, J. A. Fenger, R. Powers, G. T. Sigurdson, L. Grisanti, K. G. Guggenheim, S. Laporte, J. L. Li, T. Kondo, A. Magistrato, M. P. Moloney, M. Riley, M. Rusishvili, N. Ahmadiani, S. Baroni, O. Dangles, M. Giusti, T. M. Collins, J. Didzbalis, K. Yoshida, J. B. Siegel and R. J. Robbins, *Sci. Adv.*, 2021, **7**, eabe7871.
23 A. M. Patil, I. S. Nawghare, J. Nithyanandhan and A. V. Ambade, *Macromolecules*, 2025, **58**, 2850–2859.
24 G. Lissandrini, D. Zeppilli, F. Lorandi, K. Matyjaszewski, A. A. Isse, L. Orian and M. Fantin, *Angew. Chem., Int. Ed.*, 2025, **64**, e202424225.
25 Z. Wu, K. Jung, C. Wu, G. Ng, L. Wang, J. Liu and C. Boyer, *J. Am. Chem. Soc.*, 2022, **144**, 995–1005.
26 Q. Wang, F. Y. Bai, Y. Wang, F. Niu, Y. Zhang, Q. Mi, K. Hu and X. Pan, *J. Am. Chem. Soc.*, 2022, **144**, 19942–19952.
27 W. Hu, J. Gao, B. Shi, Z. Xia, Y. Xiao, Y. Geng and C. Lü, *ACS Catal.*, 2024, **14**, 8148–8159.
28 I. C. Anderson, D. C. Gomez, M. Zhang, S. J. Koehler and C. A. Figg, *Angew. Chem., Int. Ed.*, 2025, **64**, e202414431.
29 J. Jiang, G. Ye, F. Lorandi, Z. Liu, Y. Liu, T. Hu, J. Chen, Y. Lu and K. Matyjaszewski, *Angew. Chem., Int. Ed.*, 2019, **58**, 12096–12101.
30 M. Chen, J. Hao, W. Zhang, G. Shi, X. Zhang, Z. Cui, P. Fu, M. Liu, X. Qiao, Y. He and X. Pang, *Macromolecules*, 2022, **55**, 10788–10796.
31 C. Yu, J. Song, T. I. Kim, Y. Lee, Y. Kwon, J. Kim, J. Park, J. Choi, J. Doh, S. K. Min, S. Cho and M. S. Kwon, *ACS Catal.*, 2023, **13**, 665–680.
32 M. Zhang, J. Hao, C. Wang, Y. Zhang, X. Zhang, Z. Cui, P. Fu, M. Liu, G. Shi, X. Qiao, Y. Chang, Y. He and X. Pang, *ACS Catal.*, 2024, **14**, 16313–16323.
33 L. Zhang, X. Shi, Z. Zhang, R. P. Kuchel, R. N. Zangeneh, N. Corrigan, K. Jung, K. Liang and C. Boyer, *Angew. Chem., Int. Ed.*, 2021, **60**, 5489–5496.
34 L. Zhang, G. Ng, N. K. Kaushik, X. Shi, N. Corrigan, R. Webster, K. Jung and C. Boyer, *Angew. Chem., Int. Ed.*, 2021, **60**, 22664–22671.
35 Q. Gao, W. Wang, J. Du, Z. Liu, Y. Geng, X. Ding, Y. Chen, J. Chen and G. Ye, *Angew. Chem., Int. Ed.*, 2023, **62**, e202312697.
36 Y. Zhu, D. Zhu, Y. Chen, Q. Yan, C. Y. Liu, K. Ling, Y. Liu, D. Lee, X. Wu, T. P. Senftle and R. Verduzco, *Chem. Sci.*, 2021, **12**, 16092–16099.
37 H. Yang, R. Zhao, Z. Lu, L. Xiao and L. Hou, *ACS Catal.*, 2023, **13**, 2948–2956.
38 J. Jiang, G. Ye, Z. Wang, Y. Lu, J. Chen and K. Matyjaszewski, *Angew. Chem., Int. Ed.*, 2018, **57**, 12037–12042.
39 Y. Yu, S. Tao, Q. Zeng, Z. Ma, K. Zhang and B. Yang, *Carbon Energy*, 2025, **7**, e686.
40 X. Luo, Y. Zhai, P. Wang, B. Tian, S. Liu, J. Li, C. Yang, V. Strehmel, S. Li, K. Matyjaszewski, G. Yilmaz, B. Strehmel and Z. Chen, *Angew. Chem., Int. Ed.*, 2024, **63**, e202316431.
41 C. Zhao, H. Song, Y. Chen, W. Xiong, M. Hu, Y. Wu, Y. Zhang, L. He, Y. Liu and A. Pan, *ACS Energy Lett.*, 2022, **7**, 4389–4397.
42 Z. Xia, B. Shi, W. Zhu, Y. Xiao and C. Lü, *Adv. Funct. Mater.*, 2022, **32**, 2207655.

43 S. Shanmugam, S. Xu, N. N. M. Adnan and C. Boyer, *Macromolecules*, 2018, **51**, 779–790.
44 Q. Ma, X. Zhang, Y. Jiang, J. Lin, B. Graff, S. Hu, J. Lalevée and S. Liao, *Polym. Chem.*, 2022, **13**, 209–219.
45 C. Wu, N. Corrigan, C. H. Lim, W. Liu, G. Miyake and C. Boyer, *Chem. Rev.*, 2022, **122**, 5476–5518.
46 M. Zhao, S. Zhu, X. Yang, Y. Wang, X. Zhou and X. Xie, *Macromol. Rapid Commun.*, 2022, **43**, 2200173.
47 X. Cao, Z. Lu, H. Yang, R. Zhao, L. Xiao and L. Hou, *Polym. Chem.*, 2024, **15**, 1504–1510.
48 H. Yang, Z. Lu, X. Fu, Q. Li, L. Xiao, Y. Zhao and L. Hou, *Eur. Polym. J.*, 2022, **173**, 111306.
49 W. W. Fang, G. Y. Yang, Z. H. Fan, Z. C. Chen, X. L. Hu, Z. Zhan, I. Hussain, Y. Lu, T. He and B. E. Tan, *Nat. Commun.*, 2023, **14**, 2891.
50 S. Shanmugam, J. Xu and C. Boyer, *J. Am. Chem. Soc.*, 2015, **137**, 9174–9185.